International Journal of Fluid Machinery and Systems
Vol. 10, No. 4, October-December 2017

DOI: http://dx.doi.org/10.5293/IJFMS.2017.10.4.345
ISSN (Online): 1882-9554

Original Paper

Blade passage modeling strategy for hydraulic turbine

Ruzhi Gong[1, 2], Chirag Trivedi[2], Ole G. Dahlhaug[2] and Torbjørn K. Nielsen[2]

[1]Department of Energy Science and Engineering, Harbin Institute of Technology
No.92 West Dazhi Street, Harbin, 150001, China, gongruzhi@hit.edu.cn
[2]Department of Energy and Processing Technology, Norwegian University of Science and Technology
Alfred Getz' Vei 4, Trondheim, 7491, Norway, chirag.trivedi@ntnu.no, ole.g.dahlhaug@ntnu.no,
torbjorn.k.nielsen@ntnu.no

Abstract

CFD has played a significant role to investigate the performance and improve the design of hydraulic turbines; however, the improvement of CFD method demands powerful computer resources including time, CPU, memory, and commercial licenses. In present work, both global and local parameters of a high head Francis turbine were studied using several geometrical and interface modelling approaches. The aim of the work is to find suitable strategy for designers to simulate the hydraulic turbines to balance the numerical accuracy and the requirement of computational resources. The geometrical modelling approaches include combinations of turbine components such as, spiral casing, distributor, runner and draft tube. The interface modelling approaches includes, stage, Frozen rotor and transient rotor-stator types. The study showed that the proper combinations of both approaches can effectively reduce the numerical error.

Keywords: Hydraulic turbine, modeling strategy, pressure fluctuation, rotor-stator interaction.

1. Introduction

Greater flexibility of hydraulic machines is expected due to the development of new types of energy, but meanwhile, thinner blade is designed to achieve high efficiency. Unit availability is also a concern as there is a strong demand to move from systematic to conditional maintenance in order to reduce the downtime. More and more research has recently emphasized on the dynamic behavior of turbine. However, a large part of the design of hydraulic turbines still involves steady state simulations due to time constraints For a high head Francis turbine, both the global parameters such as efficiency, torque, etc., and local parameters including pressure fluctuations due to rotor stator interactions are important to the design. In the numerical simulations and design of hydro turbines, several efforts have been devoted [1-7].

Buron [8] used a multi-stage Runge-Kutta explicit scheme to advance the solution in time. Nonlinear harmonic (NLH) simulations are set to compute one perturbation per domain. It was shown from the results that the grid level and the computational method does not modify the mean pressure value. NLH simulations on intermediate grid level tend to overestimate the pressure amplitudes corresponding to the blade passing frequency. Jost [9, 10] claimed a new method to simulate the turbine at high load more accurately. The results of different turbulence models were compared, and concluded that Reynolds Averaged Navier-Stocks (RANS) two-equation models and Speziale-Sarkar-Gatski Reynolds stress model (SSG RSM) can predict the efficiency of the turbine quite accurately. The main reason for discrepancy between measured and calculated efficiency at full load and that is in the draft tube, where calculated flow energy losses are often overestimated. Wallimann [11] compared the pressure amplitude spectrum between measurements and simulations, the results showed that Computational Fluid Dynamic (CFD) simulations capture the relevant frequencies. The tendency of the amplitude values was correct for the point in the vaneless space compared with the experiments.

Chirag [12] reviewed the application of the numerical techniques in the simulations of hydraulic turbines. Continuous efforts have been made to improve the numerical results, but there is still a vast scope for improvement in the applied CFD techniques and turbine modeling approaches. Numerical modeling of the turbines has posed challenges over the years regarding the appropriate selection of the turbulence model, density of mesh, and boundary conditions that can provide reliable and robust results. It can be concluded that the RANS models may be considered as an optimum for the initial design phase as this approach provides a compromise between the requirements for computational cost, time, and numerical accuracy. Stoessel [13] carried out

Received February 8 2017; revised April 26 2017; accepted for publication August 10 2017: Review conducted by Prof. Minsuk Choi.
(Paper number O17001K)
Corresponding author: Ruzhi Gong, gongruzhi@hit.edu.cn

steady and unsteady simulations on a hydraulic turbine with different turbulence models. The result from the analysis showed a slight frequency shift compared to the experimental results and the expected values. The accuracy of the frequency spectrum could be improved by choosing a smaller time step and increasing the observation period. Guedes [14] investigated the behavior of the flow field in the rotor-stator zone which leads to a complex flow pattern into the stator channels. This cannot be reproduced accurately by steady state rotor-stator interaction models. The unsteady computations showed good accuracy, when compared to experimental results, displaying qualitatively the same flow features found by the measurements. In spite of that fact, the exact behavior of the machine could not be predicted in the instability zone [15, 16], this limitation can be linked to geometry modification applied to the stator domain (for example, 20 channels instead of 22) and the use of the periodicity boundary conditions. If one is interested in predicting the exact unstable behavior of the machine, a full 360-degree whole passage computation would be necessary. Hosseinimanesh[17] compared the performance of TRS (Transient Rotor Stator) and stage interface types in turbine simulations. The results showed that they have performed differently in the simulation of turbine with different water head. Zobeiri [18] validated pressure measurements performed in the guide vanes flow channels. The spectral analysis highlights that the difference stems from the pressure amplitude value of the blade passage frequency component. For the point closest to the impeller, the maximum of pressure amplitude is observed for the same component, indicating the strong influence of the potential effect in the interactions between the guide vanes and the rotating impeller blades. However, the amplitude of this component decreases very fast backward to the stay vane. Obviously, the simulations of the complete turbine will cost much more time than the single passage simulations [19].

In this work, the performance of a high head Francis turbine at Best Efficiency Point (BEP) is investigated using different methods. The main objective is to check how well the numerical methods predict the performance of the turbine because the numerical errors at this operating point are generally minimum. In this work, steady state measurements were conducted to access the turbine performance globally. The results were used to prescribe the boundary conditions and validate the numerical model. In addition, unsteady pressure measurements were conducted to investigate the ability of the strategies in capturing the RSI (Rotor Stator Interaction) phenomenon. Through the studies in the work we expect to find appropriate method for designers to simulate hydraulic turbines to balance the accuracy and the resources required, including time and computational power, in turbine calculations.

In section 2, the case studied in the present work was detailed described. In section 3, the numerical steps were provided and the measurement points were illustrated. Results of the simulations and experiments were shown in section4. At last, some conclusions were stated.

2. Case description

The experimental data used for comparison and validation in this paper were obtained from the test rig at the Waterpower laboratory, NTNU in Norway. For the discussed operation points, the test rig was operated in an open loop manner with the draft tube connected to a downstream tank. A more detailed description of the test rig and instrument can be found in [20-21]. The tested model was designed based on the prototype of Tokke power plant in Norway. The corresponding prototype values are H_P=377m, P_P=110MW, D_P=1.779m and Q_P=31m^3/s. The reference diameter of the model runner is D_2=0.349m (scale=1:5.1). The model runner consists of 15 full length and 15 splitter blades. The number of guide vanes and stay vanes is 28 and 14, respectively. Figure 1 shows the reduced scale model of the investigated Francis turbine. Experimentally, the BEP was found at H_M=11.94m, Q_M=0.199m3/s and runner speed of n_M=332.59rpm with hydraulic efficiency of η_M=92.39%.

All simulations in the present work have been conducted at BEP and the operating parameters are shown in Table1. The measurements and uncertainty quantification were conducted using the guidelines recommended in IEC60193 [22].

Table 1 Experimental operating point data for BEP (best efficiency point)

Parameter	BEP	Uncertainty (%)
Guide vane angle (α)	9.84	± 0.06°
Net head (m)	11.94	± 0.011%
Discharge (m^3 s^{-1})	0.199	± 0.13%
Torque to the generator (Nm)	616.13	± 0.03%
Friction torque (Nm)	4.52	± 1.5%
Runner angular speed (rpm)	332.59	± 0.05%
Casing inlet pressure-abs (kPa)	215.57	± 0.047%
Draft tube outlet pressure-abs (kPa)	111.13	± 0.001%
Hydraulic efficiency (%)	92.39	± 0.14%
Water density (kg m-3)	999.8	0.01%
Kinematic viscosity (m2 s-1)	9.57E-7	--
Gravity (m s-2)	9.82	--

Fig. 1 Reduced model of a high head Francis turbine.

3. Grid and numerical method

3.1 Grid and boundary conditions

The complete spiral casing with stay vanes, two guide vanes, a blade passage and complete draft tube were modeled for the numerical study. Fig 2 shows a picture of the hexahedral mesh in the turbine. The minimum angle of the mesh is 20˚ and the mesh quality in the whole turbine is higher than 0.2.

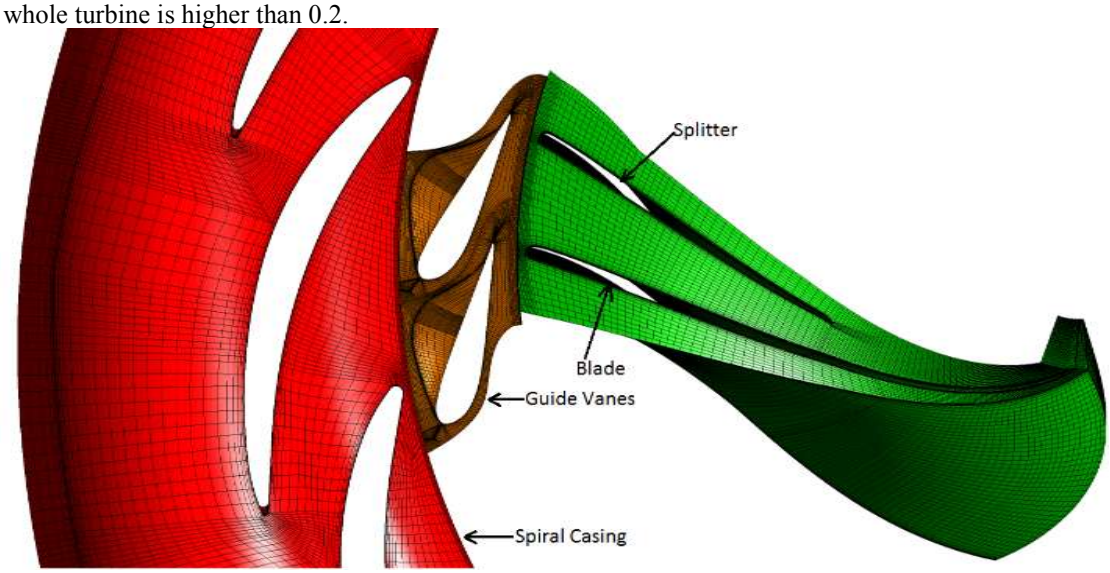

Fig. 2 Hexahedral mesh of the model Francis turbine.

Table 2 shows the mesh densities and the maximum y^+ value (at BEP) in the turbine. The fine mesh includes 28.89 million nodes for the entire turbine. The maximum y^+ value is 2.6.

Table 2 Mesh densities and y^+ information in the whole turbine.

Mesh	m_1	m_2	m_3	m_4
Nodes (million)	28.89	18.53	13.42	8.99
max y^+	2.6	29.1	164	287

Simulations were carried out using available commercial code the ANSYS^{TM} CFX^{TM} solver [23]. The stationary and rotating domains were connected through an interface modeling approach, i.e., multiple reference frames. Shear stress transport and scale-adaptive simulation (SAS) models were used for the steady-state and transient simulations, respectively. The SAS model balances the modeled and resolved parts of the turbulent stresses using a hybrid approach. It is believed that the SAS model can reproduce the unsteady phenomenon in the turbine well because SAS model will allow unsteadiness to develop [19]. However, extra fine mesh is required.

The high-resolution advection scheme was used for the current study. A second-order backward Euler scheme was applied for the time integration. The time-step size (Δt) is 0.375° of the runner. The total simulation time was equivalent to 6 revolutions of the runner. The data from the last 4 revolutions were used for analysis. Moreover, sampling points were created in the turbine to validate the local convergence.

Several parameters were used to validate the grid independency. A Richardson-extrapolation-based method, GCI [24-26], was used to estimate the discretization errors.

For the grid convergence study, the entire turbine was modeled and simulated. Table 3 shows the computed parameters using the GCI method. A representative cell size (h) for the mesh densities m_1, m_2 and m_3 is 3.6, 4.7 and 6.2 mm, respectively. The

runner torque, pressure in the vaneless space, runner and draft tube were selected to estimate the errors. The torque value represents the global performance of the turbine, whereas the pressure at specific locations represents the local performance inside the domain.

In the calculations, the grid refinement factor was computed as:

$$r_{21} = h_2 / h_1 \tag{1}$$

The extrapolated values were calculated using Eq. (2):

$$\phi_{ext}^{21} = \frac{r_{21}\phi_1 - \phi_2}{r_{21} - 1} \tag{2}$$

Then, the approximate relative error can be expressed as:

$$e_a^{21} = \left| \frac{\phi_1 - \phi_2}{\phi_1} \right| \tag{3}$$

The GCI for the fine mesh to the medium mesh is:

$$GCI_{\text{fine}}^{21} = \frac{1.25 \cdot e_a^{21}}{r_{21}^2 - 1} \tag{4}$$

Figure 3 shows the hydraulic efficiency (η_h), torque (T), head (H) and pressure (p), in the turbine for the four mesh densities. The efficiency of the turbine can be expressed as Eq. (5).

$$\eta_h = \frac{T\omega}{\rho g Q H} \quad (-) \tag{5}$$

Interestingly, the computed uncertainties (δ_{GCI}) in the local parameter (pressure) are larger than those in the global parameter (torque). This demonstrates that the computing uncertainty using a global parameter alone, which is low, is not reliable for assessing the overall performance of the turbine. The global uncertainty is 0.16%, whereas the local maximum uncertainty is 0.57%, which is computed in the runner.

Table 3 Computed discretization errors in the torque (T), pressure in the vaneless space (p_{VL}), runner (p_{R}) and pressure in the draft tube (p_{DT}). Torque values are in Nm, and pressure values are in kPa.

	m_1-m_2	h_1-h_2	r_{21}	ϕ_1-ϕ_2	ϕ_{ext}	*GCI*
T	28.89-12.85	3.6-4.7	1.31	637.9-638.4 Nm	636.4	0.16%
p_{VL1}	28.89-12.85	3.6-4.7	1.31	76.76-77.09 kPa	76.46	0.49%
p_{R1}	28.89-12.85	3.6-4.7	1.31	43.37-43.61 kPa	43.17	0.57%
p_{DT1}	28.89-12.85	3.6-4.7	1.31	5.18-5.19 kPa	5.17	0.22%

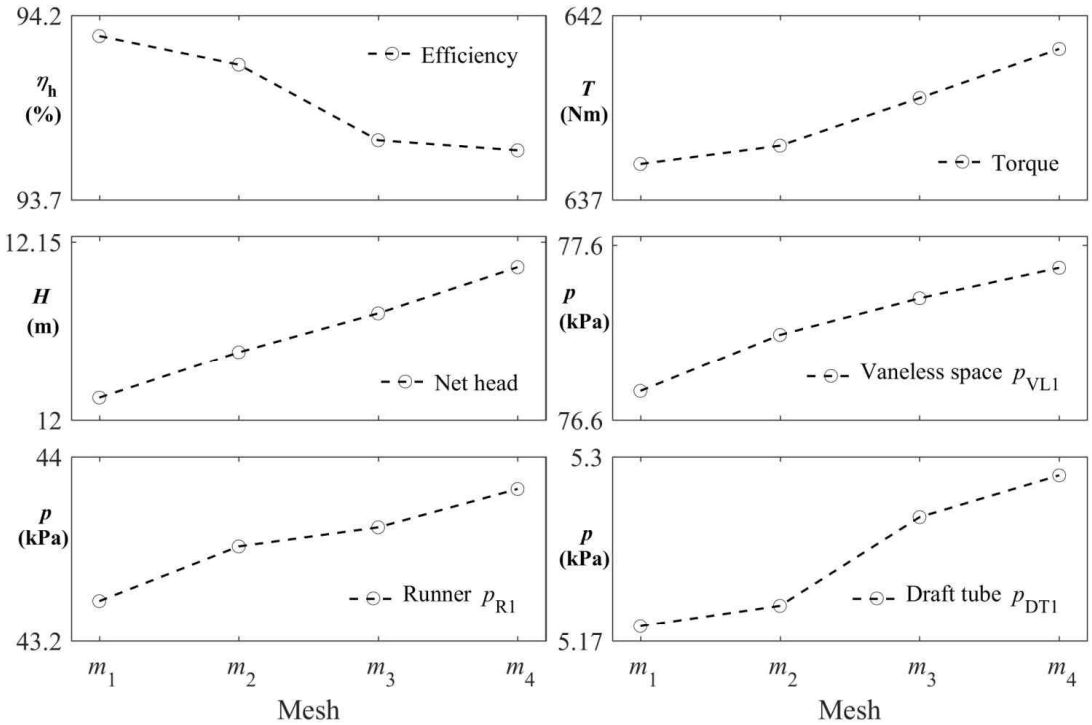

Fig. 3 Mesh convergence study of the efficiency, torque, head and pressure in the turbine. The mesh densities m_1 and m_4 correspond to 28.89 and 8.99 million nodes, respectively. The pressure in the vaneless space, runner and draft tube correspond to the point locations on the no-slip boundary.

From the above analysis for the mesh, it can be proved that the precision of the $m1$ mesh is appropriate for the calculations.

3.2 Simulation methods

Mass flow rate inlet and pressure outlet were chosen for all simulation in the work as they are most widely accepted boundary conditions for the calculation of hydraulic turbines [8-12, 18, 20, 27-28]. In the guide vane region and runner region within all simulations for the present work, periodic interface was used to simplify the model in order to save computational time. Stage interface type was used between the spiral casing and guide vane where there is no relative movement. For the connection of guide vane and runner, runner and draft tube, different interface types were used to investigate the difference among interface types, i.e. Stage in steady-state simulations, Frozen Rotor, Transient Rotor Stator and Transient Blade Row Methods in transient simulations. The minimum distance between the guide vane blade outlet and the runner blade inlet is $0.222D_2$. The radius of interface between guide vane and runner is $0.903D_2$.

Three combinations were studied in the present work: (1) guide vane and runner, (2) guide vane, runner and draft tube, (3) spiral casing, stay vane, guide vane and draft tube. For each combination, steady-state simulation, transient simulation with periodical boundary, transient simulation with Profile Transformation Method and transient simulation with Fourier Transformation Method were conducted. For the steady-state simulations, SST turbulence model was applied. For the transient simulations, SAS SST turbulence model was used except the simulations with Fourier Transformation Method because the SAS SST is not available under this condition. Instead, SST turbulence model is used. For different combinations, we used different postscripts as listed in Table 4. For the simulation methods, postscripts are listed in Table 5. Then simulations with different combination and different interface strategy can be easily defined. For instance, we use S_{1SS} represents steady-state simulation with the combinations Guide vane and Runner.

There are also some points need to be stated. For case 1, the mass flow rate was set for the runner inlet. The value of the inflow is 1/14 of the total mass flow rate of the turbine. The outlet pressure on the runner outlet was set to 0.The inflow condition for case 2 is the same as that of case 1 and the outlet pressure on the draft outlet was set to 0. Obviously those are not the exact flow condition in the turbine model. The reason why chose the above values is that the setup will not heavily influence the flow character in the turbine. However, the aim of work is to find suitable numerical modelling strategy to balance the numerical accuracy and the requirement of computational resources. For case 3, the mass flow rate on the spiral inlet was set as total flow rate of the turbine and the outlet pressure on the draft outlet was set to 0.

Table 4 Postscripts description for different combinations

Postscript	Combination
1 (case-1)	Guide vane and Runner
2 (case-2)	Guide vane, Runner and Draft tube
3 (case-3)	Spiral casing, Guide vane, Runner and Draft tube

Table 5 Postscripts description for different simulation methods.

Postscript	Simulation Method
SS	Steady state simulation
FR	Frozen Rotor interface simulation
TR	Transient Rotor Stator interface simulations
PT	simulations with Profile Transformation method
FT	Simulations with Fourier Transformation method

Several points were created to monitor the unsteady pressure fluctuation with the movement of the runner. The monitoring points are described in Figure 4. A numerical point was created at the location of the experimental pressure measurement in the vaneless space (VL3) to monitor the effects of the rotor-stator interactions. Other four points (R1, R2, R3 and R4) were created between the two runner blades to monitor the pressure fluctuation in runner region. Two points (DT5 and DT6) were created in the draft tube.

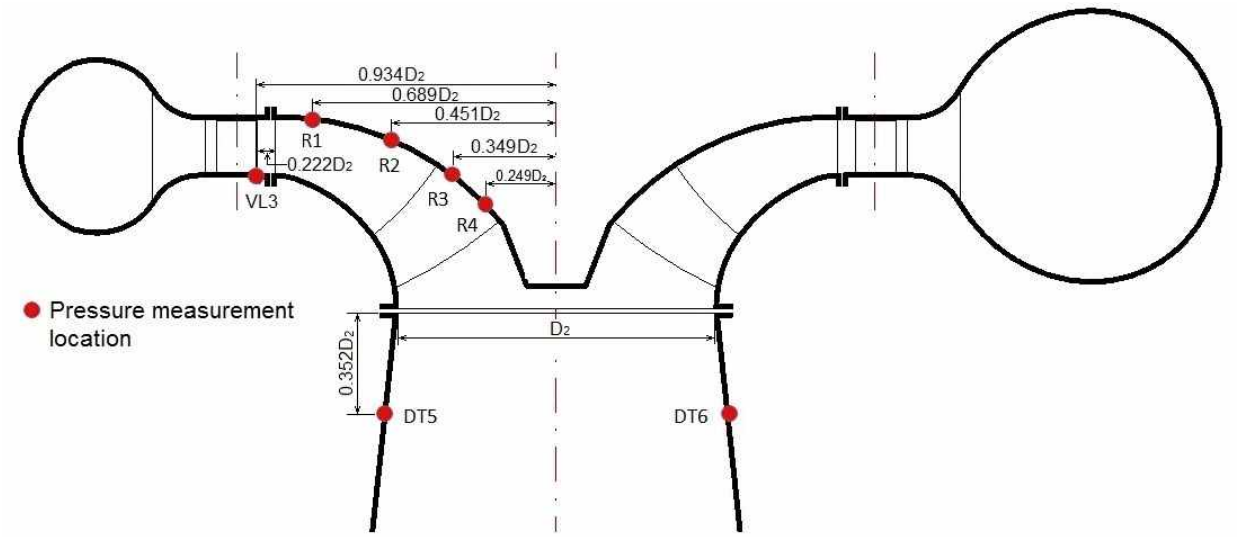

Fig. 4 Locations of pressure measurements in the turbine

4. Results and discussions

Among the combinations and interface type, of cause, case 3 will cost more time than case 2 and case1. As for steady state simulations, though they need less time than transient ones, but they actually calculate only one state of the turbine. They are only suitable for the calculation of the global parameters of the turbine, for example, head, torque and efficiency. Simulations with different interface types for the same combination need similar time to conduct the same iterations. The time needed for case 2 is about 5 times that of case 1 to run the same iterations, because case 2 has much more mesh nodes than case1 due to much larger volumn. Case 3 needs a little more time than case 2 for the same iterations. Of cause, more memory is needed for larger mesh number.

4.1 Global characteristics

Average pressure at turbine inlet and outlet were used in the calculation of turbine head (H) in steady state simulations. In transient simulations, the average values of one revolution of runner were used to calculate the turbine head and torque used in Equation (1).

Table 7 shows the performance of the turbine predicted by different combinations and methods. Equation (6) was used to determine the deviation in the table.

$$\varepsilon = \frac{\phi - \phi_{Exp}}{\phi_{Exp}} \times 100(\%) \tag{6}$$

From Table 7, we know that all combinations and methods overestimate the torque and the efficiency of the turbine, which is caused by the fact that the model and boundary conditions are ideally simplified in the simulations. Interestingly, the head of the simulation is lower than that from whole turbine simulation (12.02m) except that from steady state simulations for the case-1, and the hydraulic efficiency of the turbine is higher than that from whole turbine simulation (94.1%) except that from steady state simulation for the case-1. Single passage and periodic boundary condition were used for the guide vane and runner to be an approximation, which will lead to the ideal distribution of the pressure and velocity and will reduce the hydraulic loss in the turbine. The case-1 predicted the lowest efficiency among all the simulations because the energy recycling effect of draft tube is neglected and the inlet boundary conditions for this combination is not possible as same as that of the experiment, which means that the draft tube is very important for the efficiency of the whole turbine. The others have almost the same efficiency except the steady state ones with Stage Interface type revealing that the Stage Interface is not suitable for the connection of stationary domain and rotating domain in steady state calculations of hydraulic turbines. For the turbine head, case-1 predicted the highest ones, while the others predicted almost the same head as experiment. As for the discharge, the values and deviations were not listed because the flux rate was set as the inlet boundary condition and the final results showed the discharge deviation in the results was less than 0.2% which can be taken as numerical error. It is to say if the efficiency of the turbine is the only focus, case-2 or case-3 could be the suitable option and steady state simulations with Frozen Rotor interface type are recommended.

Table 7 Results of different combinations and methods

Combinations and Interface methods	Head (m)	Head Deviation(%)	Torque (N·m)	Torque Deviation(%)	Efficiency (%)	Efficiency Deviation(%)
Experiment	11.94	0.00	616.13	0.00	92.39	0.00
S-1SS (Stage Interface)	12.13	1.59	637.96	3.54	93.50	1.20
S-1SS (Frozen Rotor Interface)	12.09	1.26	639.85	3.85	94.09	1.84
S-1FR	11.98	0.34	639.04	3.72	94.83	2.64
S-1TR	12.08	1.17	644.89	4.67	94.89	2.71
S-1PT	12.08	1.17	645.01	6.69	94.90	2.72
S-1FT	12.10	1.34	645.21	4.72	94.79	2.60
S-2SS (Stage Interface)	11.93	-0.08	637.95	3.54	93.50	1.20
S-2SS (Frozen Rotor Interface)	11.89	-0.42	639.81	3.84	95.62	3.50
S-2FR	11.78	-1.34	639.02	3.72	96.38	4.32
S-2TR	11.88	-0.50	644.86	4.66	96.45	4.39
S-2PT	11.88	-0.50	644.97	4.68	96.46	4.41
S-2FT	11.90	-0.34	643.39	4.42	96.06	3.97
S-3SS (Stage Interface)	11.87	-0.59	638.94	3.70	95.64	3.52
S-3SS (Frozen Rotor Interface)	11.84	-0.84	641.33	4.09	96.23	4.16
S-3FR	11.82	-1.01	640.18	3.90	96.23	4.16
S-3TR	11.92	-0.17	645.32	4.74	96.22	4.15
S-3PT	11.92	-0.17	645.47	4.76	96.24	4.17
S-3FT	12.21	2.26	661.12	7.30	96.25	4.18

4.2 Local parameter analysis

Pressure fluctuations for every measurement position were obtained and Fast Fourier Transformation (FFT) method was used to study the spectral content in the pressure data. Results are provided in Figures 5-8. The frequencies were normalized by runner speed (n_R=5.543Hz). Then, a dimensionless frequency (f_b) of 15 with its harmonics was used to represent the blade passing frequency. The amplitude were normalized using Eq. (2).

$$Amplitude = \frac{A_p}{\rho g H} \times 100(\%) \quad (2)$$

Where, *Amplitude* represents the dimensionless amplitude of fluctuations and A_p represents the amplitude of fluctuations.

From the comparisons it can be indicated that the simulations with Frozen Rotor interface can't produce correct prediction for the pressure fluctuation profile for each monitoring point. Because, for the Frozen Rotor interface, the variables are averaged among the interface. It is not capable to describe the transient flow profile. All methods will underestimate the amplitude of blade passing frequency ($30f_n$) at vaneless space measurement position VL3 and runner measurement position R1.

The simulations with Transient Rotor Stator interface will produce higher frequency components for fluctuations, which do not exist in the experiments, while the simulations using Profile Transformation method and Fourier Transformation method have better performance.

Figure 5 shows the frequency domain profile of the pressure fluctuation for the measurement position VL3. All combinations and interface technologies produced the frequency of $30f_n$ which is the blade passing frequency. They all under predicted the amplitude of this frequency component. Simulations using the Fourier Transformation method produce the smallest error compared with the experiment. The frequency of $15f_n$ was also predicted correctly in the simulations, though, with higher amplitude than that from experiment. The turbine is consist of 15 complete blades and 15 splitters, which formed 15 periodical parts in the turbine runner. Therefore, the frequency of $15f_n$ is generated by the periodical geometrical feature.

Figure 6 shows the results for point R1. The blade passing frequency ($30f_n$) was captured by simulations with Transient Rotor Stator interface and simulations with Profile Transformation method. The amplitude of that frequency component was under estimated by simulations with combination of case-1, while over estimated by simulations with combinations of case-2 and case-3 with almost the same value, which indicates that the draft tube plays an important role in the pressure fluctuation inner the turbine. The frequency of $28f_n$, which has the highest amplitude at this point, was captured only by simulations with Fourier Transformation method while under predicted its amplitude. The frequency of $56f_n$, which has the second highest amplitude at this measurement point, was, also, only captured by simulations with Fourier Transformation method while, again, under predicted its amplitude. As mentioned in the model description part, 28 is the number of guide vane blade. It revealed that the flow in runner will be influenced when it is passing a guide vane blade. Interestingly, the frequency component which has the highest amplitude is not the blade passing frequency but the number of guide vane blades, which means that pressure fluctuation caused by the rotor stator interaction take the domination in runner. That is to say, the pressure fluctuation from upstream influence the flow in runner area much.

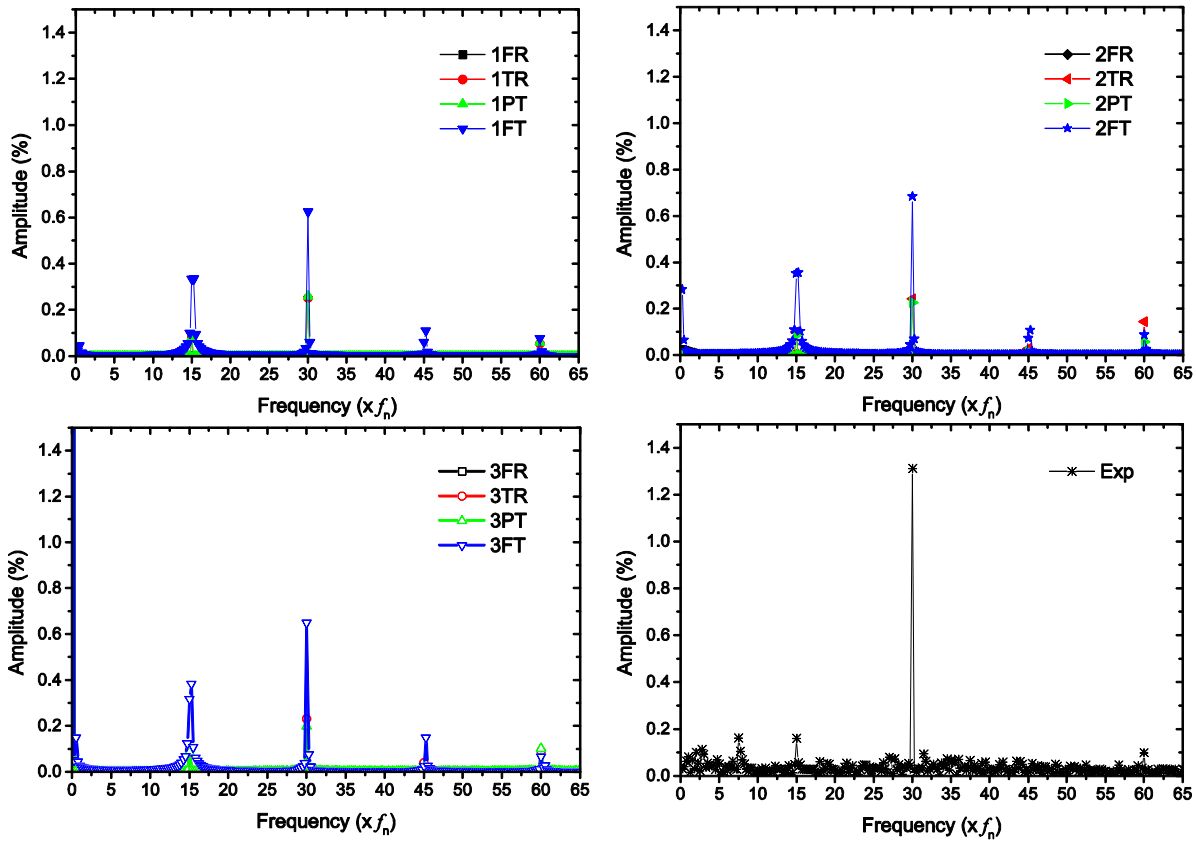

Fig. 5 Pressure profile in frequency domain for the measurement point VL3.

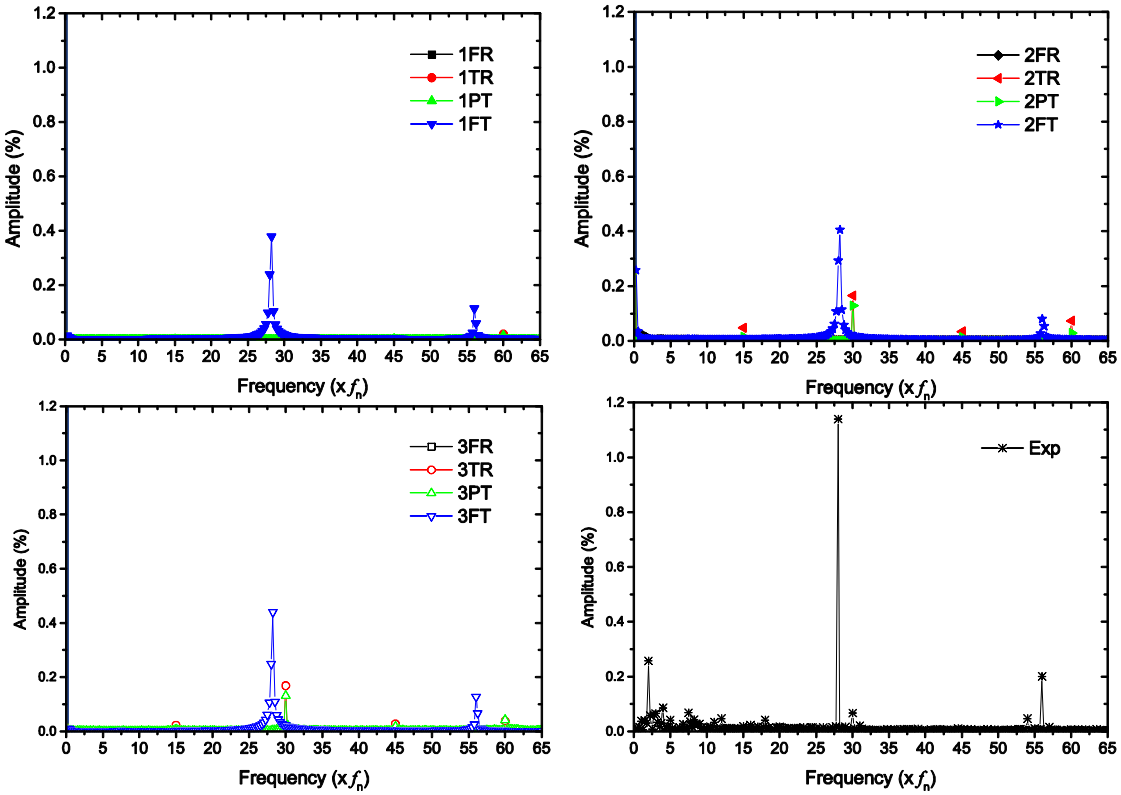

Fig. 6 Pressure profile in frequency domain for the measurement point R1.

Figure 7 shows the pressure fluctuation profile for point R4. For the blade passing frequency in this measurement point, each combination and method produced similar features as to the measurement point R1. For the frequency component of 28f_n, which has the highest amplitude at this point, Fourier Transformation method had excellent performance. Simulations with combinations of case-2 and case-3 predicted similar amplitude at this frequency to the measurement. Simulations with combinations of case-1 underestimated the amplitude at this frequency. Fourier Transformation method predicted parts of the low frequencies correctly, however, underestimate its amplitude because point R4 is close to the draft tube where the flow features are fairly complex.

From the analysis of Figure4-Figure7, it can be implied that the pressure fluctuations in one part will not influenced by motion of itself but mostly by RSI from the nearest part. For example, the pressure fluctuations in vaneless area are mostly influenced by runner. However, the pressure fluctuations in runner are mostly influenced by guide vane, however.

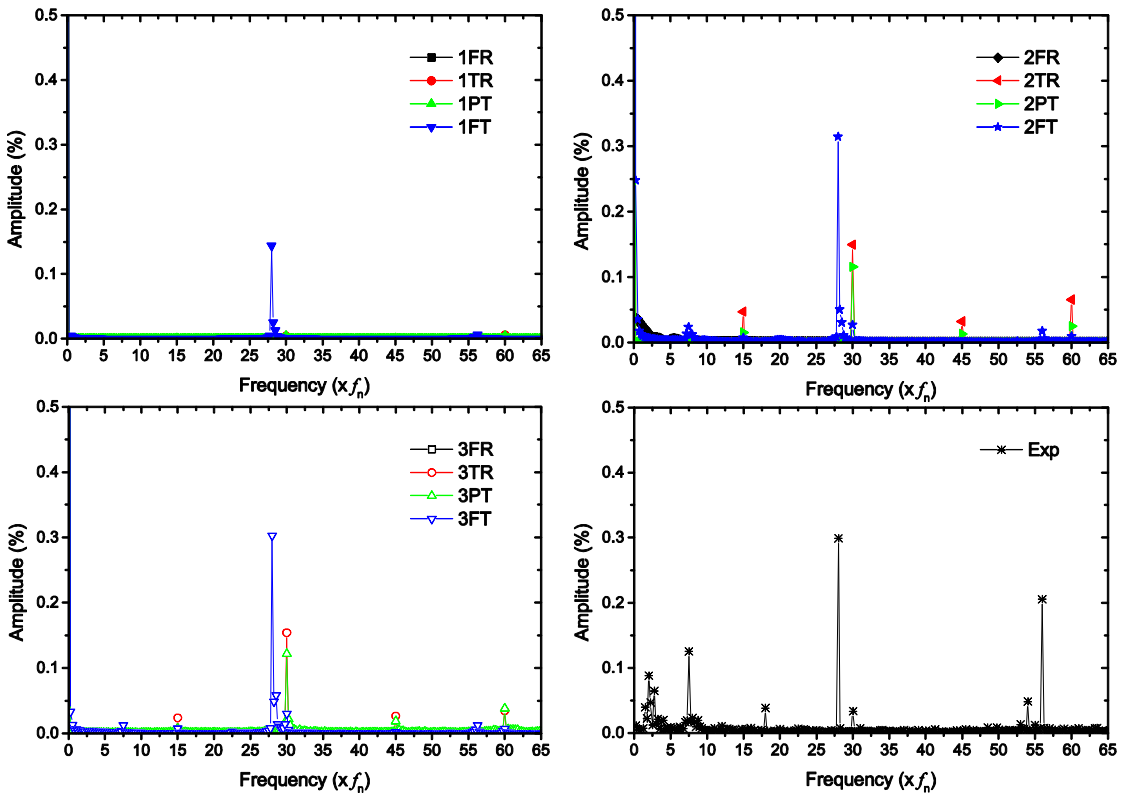

Fig. 7 Pressure profile in frequency domain for the measurement point R4.

It is hard to reproduce the pressure profile in the draft tube because the flow feature in draft tube is complex. Figure 8 shows that all combinations and methods studied in present work failed to predict the pressure fluctuation profile in draft tube accurately. Possibly, the whole turbine simulations are expected if the main focus is the flow in the draft tube.

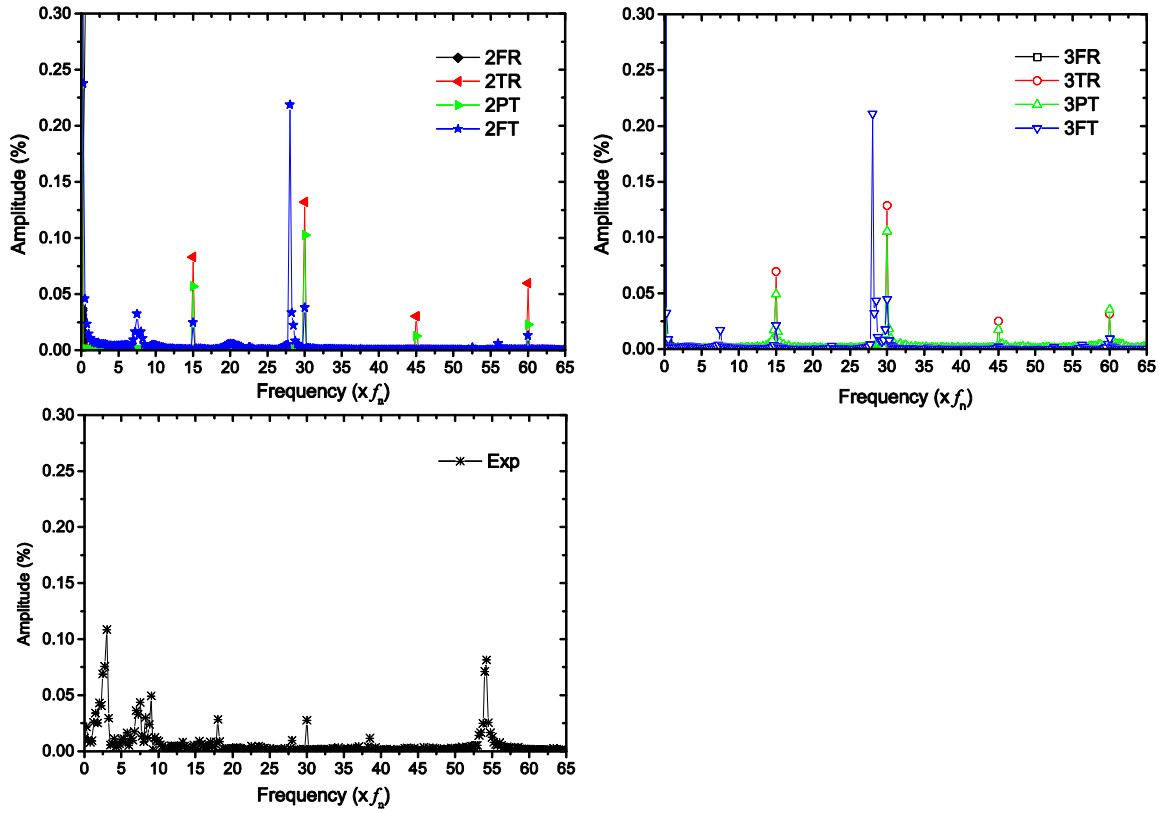

Fig. 8 Pressure profile in frequency domain for the measurement point DT5.

As we noticed that, there are frequencies about 2.5*f*n and 7.5 *f*n in Figure5-Figure8. They are standing waves originated from overhead tank and draft tube tank respectively. That is to say, these frequencies are not generated by the turbine itself. Therefore, simulations cannot capture these frequencies.

From simulations and analysis above, we know that the Fourier Transformation method has better performance than the other interface modeling strategies in the prediction of pressure fluctuations inside the turbine. It can be concluded from the contrast of the results of different combinations that the draft tube affects the pressure fluctuations in the turbine greatly. While the spiral case has less influence on the predictions.

5. Conclusion

In this study, the single passage of the guide vane and the single passage of runner are used for the simulations. Obviously, this will save a lot of time and other computing resources, such as time, memory and so on.

The simulations overestimates the efficiency of the turbine. This is because the mechanical losses in the machine are neglected. The efficiency predicted is higher than that from a similar simulation using the whole turbine. This is due to the single passage and periodic boundary conditions that were used for the guide vane and runner as an approximation, which leads to an ideal distribution of the pressure and velocity and it reduces the hydraulic loss in the turbine.

In addition, the Frozen Rotor interface is recommended for the connection of the stationary and rotation part in the steady state simulations for smaller error.

In the simulations and experiments, we noticed that rotor stator interaction dominates the pressure fluctuations in the vaneless space and runner region. The pressure fluctuations in one part will not influenced by motion of itself but mostly by RSI from the nearest part. For example, the pressure fluctuations in vaneless area are mostly influenced by runner. However, the pressure fluctuations in runner are mostly influenced by guide vane. The Fourier Transformation method has better performance for the pressure fluctuation prediction, than the other interface modeling strategies. It is a best option if we can't afford the cost of whole turbine simulations.

The draft tube affect both global and local parameters in the turbine, so it should be included in all kinds of turbine calculations. In contrast, spiral casing has less influence on the performance of the turbine. However, if the focus of the study is the detailed flow features inside the turbine in or nearby the spiral casing, the spiral casing should be included. For example, when we focus on the velocity distribution inner guide vane domain, the inlet boundary condition (within the inlet of guide vane domain) could not have an accurate input without spiral casing. Then, whole turbine simulations are suggested.

References

[1] Vu, T. C., Shyy, W., 1990, “Viscous flow analysis as a design tool for hydraulic turbine components,” ASME Journal of fluid engineering, Vol.112, pp. 5-11

[2] Sick, M., Casey, M. V., 1996, “Galphin P F. Validation of a stage calculation in a Francis turbine,” 18th IAHR Symposium Hydraulic Machinery and Cavitation, Valencia.

[3] Peng, G. Y., Cao, S. L., Ishizuka, M., and Hayama, S., 2002, “Design optimization of axial flow hydraulic turbine runner: Part I—an improved Q3D inverse method,” International journal for numerical methods in fluids, Vol.39, pp. 517-531

[4] Peng, G. Y., Cao, S. L., Ishizuka, M., and Hayama, S., 2002, “Design optimization of axial flow hydraulic turbine runner Part II—multi-objective constrained optimization method,” International journal for numerical methods in fluids, Vol. 39, pp. 533-548

[5] Peng, G. Y., 2005, “A practical combined computation method of mean through flow for 3D inverse design of hydraulic turbomachinery blades,” ASME Journal of fluid engineering, Vol. 127, pp. 1183-1190

[6] Wu, Y. L., Liu, S. H., Dou, H. S., and Zhang, L., 2011, “Simulations of unsteady cavitating turbulent flow in a Francis turbine using the RANS method and the improved mixture model of two-phase flows,” Engineering with Computers, Vol. 27, pp. 235–250

[7] Amstutz, O., Aakti, B., Casartelli, E., Mangani, L., and Hanimann, L., 2015, “Predicting the performance of a high head Francis turbine using a fully implicit mixing plane,” Journal of Physics: Conference Series, Vol. 579, p. 012009

[8] Buron, J. D., Houde, S., Lestriez, R., and Deschênes, C., 2015, “Application of the non-linear harmonic method to study the rotor-stator interaction in Francis-99 test case,” Journal of Physics: Conference Series, Vol. 579, p. 012013

[9] Jost, D., Škerlavaj, A., and Lipej, A., 2012, “Numerical flow simulation and efficiency prediction for axial turbines by advanced turbulence models,” IOP Conf. Series: Earth and Environmental Science, Vol. 15, p. 06201

[10] Jost, D., Skerlavaj, A., Morgut, M., Meznar, P., and Nobile, E., 2015, “Numerical simulation of flow in a high head Francis turbine with prediction of efficiency, rotor stator interaction and vortex structures in the draft tube,” Journal of Physics: Conference Series, Vol. 579, p. 012006.

[11] Wallimann, H., and Neubauer, R., 2015, “Numerical Study of a High head Francis turbine with measurements from the Francis-99 Project,” Journal of Physics: Conference Series, Vol. 579, p. 012003

[12] Trivedi, C., Cervantes, M. J., and Dahlhaug, O. G., 2016, “Numerical techniques applied to hydraulic turbines-A perspective Review,” ASME Transactions: Applied Mechanics Reviews, Vol. 68, p. 010802-1

[13] Stoessel, L., Nilsson, H., 2015, “Steady and unsteady numerical simulations of the flow in the Tokke Francis turbine model, at three operating conditions,” Journal of Physics: Conference Series, Vol. 579, p. 012011

[14] Guedes, A., Kueny, J. L., Ciocan, G. D., and Avellan, F., 2002, “Unsteady rotor-stator analysis of a hydraulic pump-turbine-CFD and experimental approach,” 21st IAHR Symposium on Hydraulic Machinery and Systems, Lausanne, Switzerland

[15] Trivedi, C., Cervantes, M. J., and Dahlhaug, O. G., 2016, “Experimental and Numerical Studies of a High-Head Francis Turbine: A Review of the Francis-99 Test Case.,” Energies, Vol. 9, No. 2, p. 00074

[16] Trivedi, C., Cervantes, M. J., and Gandhi, B. K., 2016, “Numerical Investigation and Validation of a Francis Turbine at Runaway Operating Conditions,” Energies, Vol. 9, No. 3, p. 00149.

[17] Hosseinimanesh, H., Devals, C., Nennemann, B., Reggio, M., and Guibault, F., 2017, “A numerical study of Francis turbine operation at no-load condition,” ASME Journal of fluid engineering, Vol. 139, p. 011104-1

[18] Zobeiri, A., Kueny, J. L., Farhat, M., and Avellan, F., 2006, “Pump-turbine Rotor-Stator Interactions in Generating Mode: Pressure Fluctuation in Distributor Channel,” 23rd IAHR Symposium on Hydraulic Machinery and Systems, Yokohama, Japan

[19] Nicolle, J., and Cupillard, S., 2015, “Prediction of dynamic blade loading of the Francis-99 turbine,” Journal of Physics: Conference Series, Vol. 579, p. 012001.

[20] Trivedi, C., Cervantes, J. M., Gandhi, B. K., and Dahlhaug, O. G., 2013, “Experimental and Numerical Studies for a High Head Francis Turbine at Several Operating Points,” ASME Journal of Fluids Engineering, Vol. 135, p. 111102.

[21] Trivedi, C., 2014, "Experimental and Numerical Investigations on Steady State and Transient Characteristics of a High Head Model Francis Turbine," Ph. D. Thesis, Indian Institute of Technology, Roorkee.

[22] IEC 60193 1999-11 IEC Hydraulic Turbines, Storage Pumps and Pump-Turbines – Model acceptance tests International Electrotechnical Commission

[23] ANSYS User Manual, 2012, ANSYS CFX Release 12.1 Canonsburg, PA.

[24] Celik, I. B., Ghia, U., and Roache, P. J., 2008, “Procedure for estimation and reporting of uncertainty due to discretization in CFD applications,” ASME Journal of Fluid Engineering, Vol. 130, p. 078001.

[25] Vu, T. C., Devals, C., Zhang, Y., Nennemann, B., and Guibault, F,. 2011, “Steady and unsteady flow computation in an elbow draft tube with experimental validation,” International Journal of Fluid Machinery and Systems, Vol. 4, Issue 1, pp. 85-96.

[26] Page, M., Beaudoin, M., and Giroux, A, M., 2011, “Steady-state Capabilities for Hydroturbines with OpenFOAM,” International Journal of Fluid Machinery and Systems, Vol. 4, Issue 1, pp. 85-96.

[27] Zhao, Y. P., Liao, W. L., Ruan, H., and Luo, X. Q., 2015, “Performance study for Francis-99 by using different turbulence models,” Journal of Physics: Conference Series, Vol. 579, p. 012012.

[28] Mossinger, P., Jester-Zurker, R., and Jung, A., 2015, “Investigation of different simulation approaches on a high-head Francis turbine and comparison with model test data: Francis-99,” Journal of Physics: Conference Series, Vol. 579, p. 012005.